Preprint
UCRL-JC-147402

Hohlraum-Driven High-Convergence Implosion Experiments with Multiple Beam Cones on the Omega Laser Facility

P.A. Amendt, R.E. Turner, and O.L. Landen

This article was submitted to
Physical Review Letter

February 22, 2002

Hohlraum-driven high-convergence implosion experiments with multiple beam cones on the Omega laser facility

Peter Amendt, R.E. Turner and O.L. Landen
Lawrence Livermore National Laboratory, Livermore, California 94550

High-convergence implosion experiments have been performed on the Omega laser facility [T.R. Boehly *et al.*, Opt. Commun. **133**, 495 (1997)] using cylindrical gold hohlraums with 40 drive beams arranged into multiple cones. These experiments make use of improved hohlraum radiation symmetry conditions [T.J. Murphy *et al.*, Phys. Rev. Lett. **81**, 108 (1998)] to demonstrate repeatably high, near one-dimensional (spherical), primary neutronic performance of single-shell implosions with measured deuterium fuel convergences approaching 20.

PACS numbers: 52.40.Nk, 52.50.Jm, 52.58.Ns

The goal of inertial confinement fusion (ICF) is to implode a capsule filled with deuterium-tritium to a sufficient density and temperature for achieving thermonuclear ignition and energy gain [1]. In the indirect-drive option, a capsule is placed at the center of a hollow high-Z radiation enclosure or hohlraum which converts absorbed laser rays into x rays that ablate the outside of the fuel-filled capsule and drive an implosion. A necessary requirement for ignition of the fuel is that the x-ray flux symmetry have satisfactory uniformity to achieve a nearly symmetric implosion. The National Ignition Facility (NIF) [2] is planned to demonstrate ignition under hohlraum conditions where the RMS time-integrated flux non-uniformities are <2% for the 16 ns duration of the laser drive [3]. A further requirement on the flux symmetry is that time-dependent asymmetry excursions not exceed 5-10% over any 3 ns interval in the drive [3]. Given these symmetry constraints on the NIF an experimental effort on the University of Rochester's Omega laser [4] is in place to diagnose and control hohlraum symmetry conditions as a prelude to the NIF.

Time-integrated x-ray symmetry control has been demonstrated on the Omega laser [5] using a NIF-like multicone geometry [Fig. 1]. Twenty beams distributed over three cones (5, 5, 10) enter each end of the gold hohlraum through a laser-entrance-hole (LEH) at three distinct angles to the hohlraum symmetry axis: θ=21.4, 42, and 58.9°. The laser energy of 0.351 nm wavelength is absorbed by the gold hohlraum walls and the energy is efficiently reradiated as a quasi-Planckian spectrum of x rays. Analysis and simulations show that high-spatial frequency x-ray drive variations are effectively smoothed as the radiation is transported from the hohlraum wall to the capsule surface. The degree of flux symmetrization improves as the hohlraum case-to-capsule ratio is increased, but at the expense of reduced energy absorbed by the capsule. The baseline NIF target design uses a hohlraum case-to-capsule ratio of 2.5 and delivers 150 kJ of

energy to the capsule compared to 1.8 MJ of available laser energy [3]. For such a moderate case-to-capsule ratio low spatial-frequency drive variations are not effectively smoothed by radiation transport alone and alternative methods must be implemented. The symmetry-control techniques envisioned for the NIF include (1) using multiple beam cones per side, (2) using hohlraum gasfills to limit the spatial excursions of the laser absorption regions or "hot spots", (3) changing the relative power (via "beam phasing") between the inner and outer laser cones for dynamic symmetry control, and (4) using high-Z mixtures in the hohlraum wall for reducing the x-ray emissivity contrast between the unirradiated wall and the laser hot spots [6].

The hohlraum symmetry effort on Omega has focussed to date on meeting the required symmetry criteria for a NIF-like case-to-capsule ratio by exploiting the first technique, i.e., use of the multicone geometry [5,7]. Recent studies have confirmed a large improvement in capsule performance on Omega for moderate convergence ($\approx$9) indirectly-driven capsules [8] compared to its 10 beam, single-cone predecessor - the Nova laser [9]. Here, we define convergence as the initial fuel radius divided by the imploded fuel radius. A useful figure-of-merit for implosion performance is the ratio of the measured primary {D+D$\rightarrow$n(2.45MeV)+He^3(0.82MeV)} neutron yield divided by the simulated one-dimensional (1D) "clean" neutron yield (YoC). A clean yield refers to the calculated neutron yield excluding the performance degrading effects of hydrodynamic instability. On Nova the YoCs for moderate convergence implosions were typically about 25% [10], whereas on Omega the YoC's are about three times larger [8]. The four reasons for this demonstrated improvement are ascribed to (1) the factor-of-three reduction in time-dependent lowest-order (2^{nd} Legendre) flux asymmetry swings inherent to the multicone geometry [8], (2) the reduced time-integrated 4^{th} Legendre distortion also inherent to the multicone geometry [8], (3) the greater azimuthal flux symmetry arising from having on average 2$\times$ more beams/cone, and (4) the 2$\times$ reduction in random flux asymmetries due to having 4$\times$ more beams with similar beam-to-beam power balance.

In this Letter we exploit the improved hohlraum symmetry conditions on Omega to demonstrate high-convergence implosions for a NIF-relevant case-to-capsule ratio of $\approx$3. The reported high convergences ($\approx$20) are directly inferred from secondary {D+T(<1.01MeV)$\rightarrow$n(11.8-17.1MeV)+He^4} neutron measurements with the Medusa detector [11] which provide a sensitive indicator of the compressed fuel areal density [12]. This result represents a factor-of-two improvement in the highest observed convergence to date of an indirectly-driven single-shell capsule for a NIF-like case-to-capsule ratio. Similar high convergences have been reported previously with indirect drive but either under conditions of large case-to-capsule ratio (>6) for

flux asymmetry mitigation on Nova [13] or in double-shell experiments on Omega where the fuel convergence is generously defined relative to the *outer* shell radius [14].

Figure 1 shows the Omega hohlraum geometry used for our high-convergence implosion studies. The "scale-1" thinwall gold hohlraums were 2400 μm long with a radius of 800 μm and 600 μm radii LEHs. The hohlraum wall consisted of 2 μm of Au overcoated with 50 μm of epoxy to accommodate noninvasive x-ray imaging of the fuel-pusher region at peak x-ray emission. The laser beams were positioned along the hohlraum symmetry axis to give the best time-integrated lowest-order flux symmetry at the capsule. The capsule was a CH (plastic) shell of nominal 30 μm thickness and inner radius of 220 μm. The shell is doped with 1% Ge to mitigate volumetric x-ray preheat above the n=2 bound-free absorption edge of Ge (1.2 keV). Deuterium (D_2) is used as the fuel fill and the convergences are varied by adjusting the room temperature fuel pressure between 5 and 50 atm.

Figure 2 shows the laser power history used to drive the hohlraums. The nominal energy of 14 kJ is delivered within 2.5 ns and uses a two-step pulse shape for efficient compression of the fuel. Also shown is the measured and calculated x-ray drive history as seen by Dante (15), an array of x-ray diodes positioned at 37° to the hohlraum axis outside the LEH [See Fig. 1]. The calculations are based on integrated hohlraum radiation-hydrodynamics simulations [16] and post-processed to simulate the Dante view of the hohlraum wall and laser hot-spots through the LEH [17]. The agreement between the measured and calculated drive temperature is very close and suggests weak levels of backscatter losses which have not been included in the simulations. Indeed, full-aperture backscatter (FABS) measurements on (outer) cones 2 and 3 show total backscatter levels into the f/6 lens cones generally less than 200 J; near backscatter outside of the monitoring lenses is estimated to be at a similar level based on near backscatter imaging (NBI) experience on Nova [18]. Cone 1 FABS monitoring is not yet available on Omega but comparison of the length of hohlraum plasma traversed and wall intensity with the geometry of cone 2 argues for a total cone 1 backscatter level of ≈200 J. Thus, we infer a total backscatter level of only 600 J or 4% of the incident laser energy, corresponding to an imperceptible 3 eV deficit in peak drive temperature.

Measured peak x-ray emission times from the imploded core provide a further check on the hohlraum drive. Figure 3 shows a comparison of the measured and simulated peak x-ray emission times for the three capsule types. The good agreement verifies that the hohlraum drive is properly modeled in the calculations which is a prerequisite for reliably simulating implosion performance.

The traditional figure-of-merit for modeling ICF implosion performance is the ratio of observed primary (DD) neutron yield to the simulated DD neutron yield. Figure 4(a) shows the measured DD neutron yields, normalized to calculated clean DD neutron yields from two-dimensional (2D) integrated hohlraum simulations [19], versus the measured fuel convergence. The convergence is inferred from the ratio of secondary (DT) neutron yield, as recorded by a time-resolved neutron sensitive scintillator array - Medusa [11], to the DD neutron yield. Specifically, the measured DT/DD neutron ratio determines the fuel areal density $\langle \rho R \rangle$ and hence, by conservation of fuel mass, the convergence through use of a "hot spot" model [12] and accounting for triton slowing in a 1 keV plasma. The hot spot model assumes that all primary reaction products are created at the center of a spherical fuel volume with uniform temperature and density. Figure 4(a) shows that the highest convergence targets at 5 atm D_2 fill had a mean YoC_{2D} performance near 30%, including the effects of intrinsic hohlraum (2D) flux asymmetry. Calculations that gauge the degradation from resolvable long-wavelength radiation asymmetries alone show a 25% yield degradation for 50 atm D_2 fill capsules and over 50% for the 5 atm capsules.

To explain the residual degradation in performance indicated in Fig. 4(a) we have used a Haan-type mix analysis [20] to assess the role of Rayleigh-Taylor instability at the fuel-pusher interface. Calculations suggest that perturbations on this interface are primarily seeded by feedthrough of outer surface perturbations during shock transit. Each target was measured for outer surface roughness and the resulting power spectrum was convolved with a calculated linear growth factor spectrum to generate a time-dependent mode spectrum on the inner surface of the shell. For each type of capsule we calculated the linear growth factor spectrum and found peak values, defined as the final-to-initial amplitude, in excess of 200. The 5- and 10-atm D_2-filled capsules both attain maximum growth near $\ell_{max} \approx 20$ while for the low convergence capsule, $\ell_{max} \approx 30$, where ℓ is the Legendre mode number of the surface perturbation. For comparison, the expected growth factor on the NIF is 400-1000 [1]. The Haan prescription for weakly nonlinear saturation is applied and the resulting spectrum of modes is summed in quadrature to generate a time-varying mix region. The yield degradation in a 1D simulation with a dynamic mix layer is then multiplicatively applied to a clean 2D integrated hohlraum simulation prediction to estimate the combined effect of mix and intrinsic radiation asymmetry on DD neutron performance. Figure 4(b) shows the result of this procedure applied to the three types of capsule. The performance of the low convergence targets matches well the predicted DD neutron yields according to our prescription for degradation from mix and flux asymmetry. Other sources of

degradation such as long-wavelength capsule nonuniformities and random flux asymmetry from laser power imbalances exist but are estimated to contribute less than 10% in total. For the higher convergence targets Fig. 4(b) shows that only a 20-30% margin for yield degradation is left. Here, the effects of a plausible 0.5 μm ℓ=1 shell thickness variation alone can contribute a 20% degradation in yield [21].

Multiple 4-6 keV x-ray images of the imploded cores were obtained using an array of 5 μm pinholes and 70 ps resolution framing cameras. Figure 5(a) shows the comparison between the measured and expected 50% self-emission contour sizes for fuel Bremsstrahlung x rays. This contour correlates well with the fuel-pusher interface for the higher convergence capsules, i.e., 5 and 10 atm D_2-fill, according to the simulations. For the lowest convergence capsules, i.e., 50 atm D_2-fill, the core conditions are (2.5×) less isothermal, giving more localized emission at the core and a less reliable indicator of fuel size based on a 50% x-ray self-emission contour. A lower intensity contour could be chosen to better match the location of the fuel-pusher interface, but such an exercise is intrinsically model-dependent and illustrates the disadavantage of inferring a fuel convergence from x-ray core imaging alone [14, 22]. Figure 5(b) shows the measured distortions of the 50% emission contour versus inferred convergence from secondary neutron measurements. The standard metric for core distortion is "*a/b*", where *a* (*b*) is the radius of the 50% contour along the hohlraum waist (axis). The shaded region corresponds to an allowed core distortion for a NIF-relevant RMS time-integrated lowest-order flux asymmetry of <2%. Overall, the data show effective symmetry control at the highest convergences near the level required for the NIF.

In summary, we have demonstrated repeatable, near 1D performance of hohlraum-driven high-convergence (≈20) single-shell implosions with the Omega laser using a NIF-like hohlraum geometry. The demonstrated laser power balance and radiation uniformity have satisfactorily reduced the sources of random and intrinsic (ℓ=2, 4) flux asymmetry to levels required for demonstrating ignition on the NIF. Demonstration of even higher ignition-relevant convergences (>30) via secondary neutron measurements is not considered possible with the Omega laser due to the energy limitations (≈20 kJ). For example, the same CH capsule filled with only 2 atm of D_2 is predicted to reach a convergence greater than 30 according to (clean) 1D simulations, but the sampling errors for secondary neutron detection become too large for reliably inferring a fuel convergence. Instead, x-ray core imaging techniques become the lone option [14,22], but with the attendant disadvantage that an inferred fuel convergence becomes significantly model-dependent.

We acknowledge useful discussions with Steve Haan, Bruce Hammel, John Lindl and Larry Suter. We are indebted to Russ Wallace for target fabrication and to the Omega team for operational support. This work was performed under the auspices of the U.S. Department of Energy by the Lawrence Livermore National Laboratory under Contract No. W-7405-Eng-48.

This work was performed under the auspices of the U.S. Department of Energy by the University of California, Lawrence Livermore National Laboratory under Contract No. W-7405-Eng-48.

Figure Captions

Fig. 1: Schematic of hohlraum geometry and Omega laser cone configurations with indicated diagnostic lines-of-sight.

Fig. 2: Measured (filled squares) and simulated (solid line) Dante drive temperature versus time; laser power history (dashed-dotted) versus time.

Fig. 3: Measured versus simulated instant of peak x-ray self-emission for 5 atm D_2-filled capsules (open squares), 10 atm D_2-filled capsules (filled circles), and 50 atm D_2-filled capsules (open circles).

Figs. 4(a-b): (a) Ratio of measured primary (DD) neutron yield over clean 2D simulated yield versus inferred fuel convergence from secondary (DT) neutrons for 5 atm D_2-filled capsules (open squares), 10 atm D_2-filled capsules (filled circles), and 50 atm D_2-filled capsules (open circles). Bold symbols denote averaging over each target type. (b) Averaged ratio of measured primary (DD) neutron yield to 2D simulated yield with 1D mix model versus inferred fuel convergence from secondary (DT) neutrons.

Figs. 5(a-b): (a) Measured versus simulated average radius of 50% x-ray self-emission contour; (b) measured and simulated "*a/b*" distortion of 50% x-ray self-emission contour versus inferred fuel convergence for 5 atm D_2-filled capsules (open squares), 10 atm D_2-filled capsules (filled circles), and 50 atm D_2-filled capsules (open circles); simulation points are indicated in gray.

References

[1] J.D. Lindl, Inertial Confinement Fusion (*Springer-Verlag, New York, 1998*).

[2] J.A. Paisner *et al.*, Laser Focus World **30**, 75 (1994).

[3] S.W. Haan *et al.*, Phys. Plasmas **2**, 2480 (1995).

[4] T.R. Boehly *et al.*, Opt. Commun. **133**, 495 (1997).

[5] T.J. Murphy *et al.*, Phys. Rev. Lett. **81**, 108 (1998).

[6] L.J. Suter *et al.*, Phys. Plasmas **7**, 2092 (2000).

[7] R.E. Turner *et al.*, Phys. Plasmas **7**, 333 (2000).

[8] R.E. Turner *et al.*, in preparation (2002).

[9] E.M. Campbell, Laser Part. Beams **9**, 209 (1991).

[10] M.M. Marinak *et al.*, Phys. of Plasmas **3**, 2070 (1996).

[11] J.P. Knauer *et al.*, Rev. Sci. Instrum. **66**, 926 (1995).

[12] H. Azechi, M.D. Cable, and R.O. Stapf, Laser Part. Beams **9**, 119 (1991).

[13] M.D. Cable *et al.*, Phys. Rev. Lett. **73**, 2316 (1994).

[14] W.S. Varnum *et al.*, Phys. Rev. Lett. 81, 5153 (2000).

[15] H.N. Kornblum, R.L. Kauffman, and J.A. Smith, Rev. Sci. Instrum. **57**, 2179 (1986).

[16] G.B. Zimmerman and W.L. Kruer, Comments Plasma Phys. Control. Fusion **2**, 51 (1975).

[17] C. Decker *et al.*, Phys. Rev. Lett. **79**, 1491 (1997).

[18] R.K. Kirkwood *et al.*, Rev. Sci. Instrum. **68**, 636 (1997).

[19] L.J. Suter *et al.*, Phys. Rev. Lett. **73**, 2328 (1994).

[20] S.W. Haan, Phys. Rev. A **39**, 5812 (1989).

[21] J.D. Lindl *et al.*, Phys. Plasmas (submitted).

[22] J.M. Wallace *et al.*, Phys. Rev. Lett. **82**, 3807 (1999).

Fig. 1

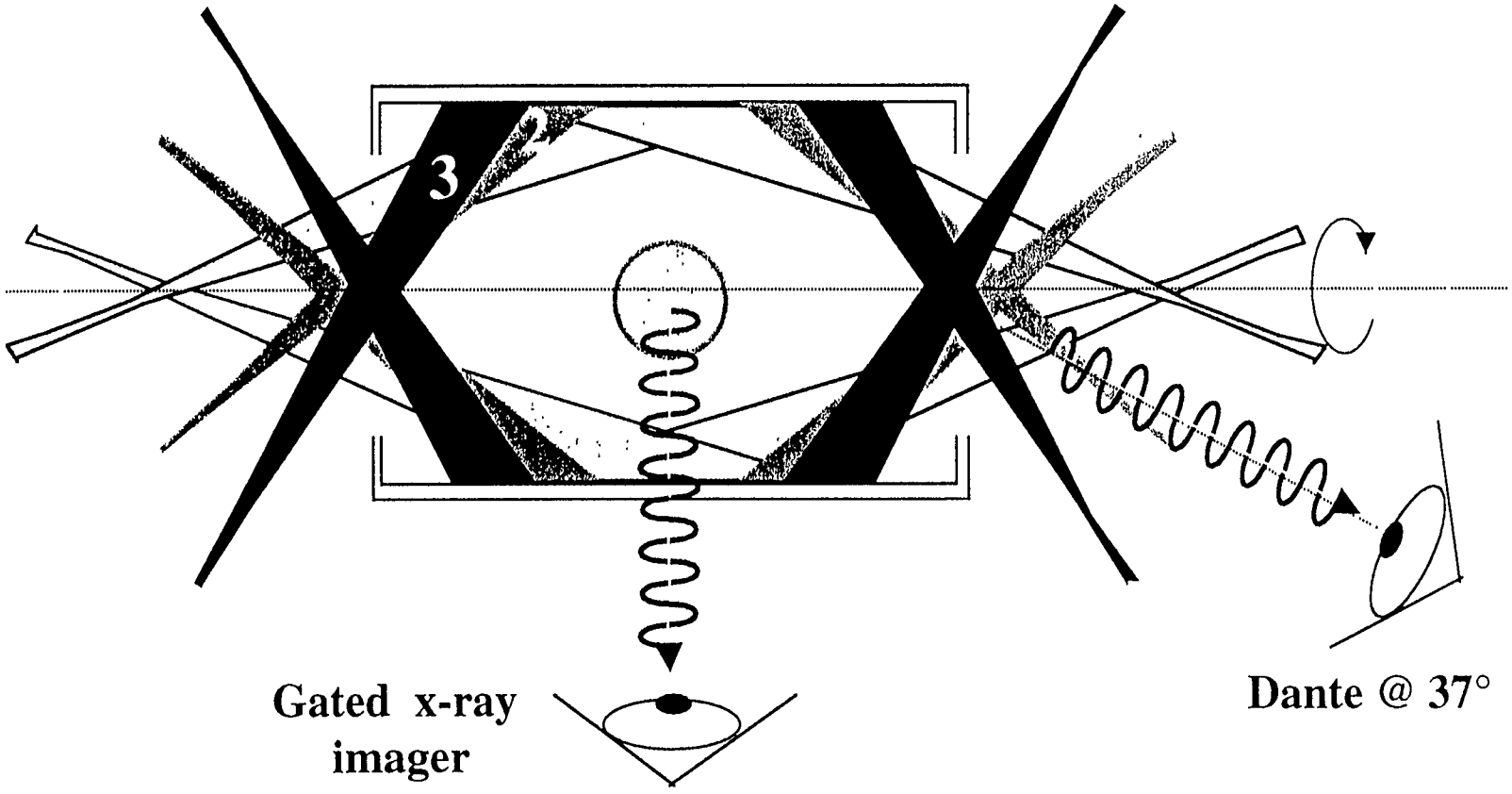

Fig. 2

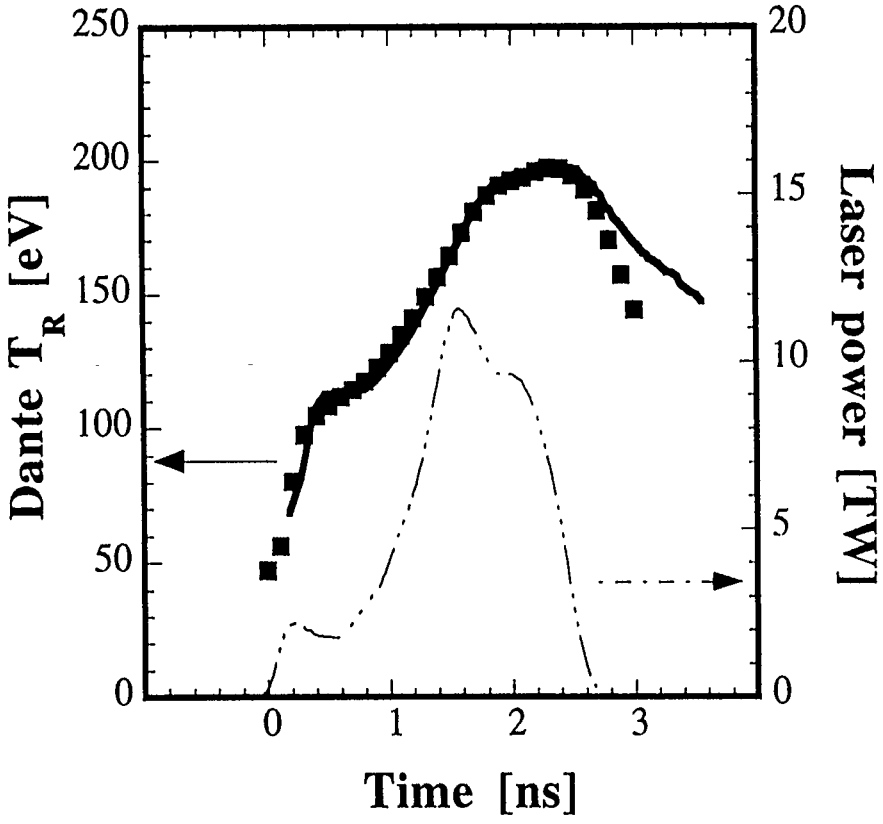
250
200
150
100
50
0
Dante T_R [eV]
20
15
10
5
0
Laser power [TW]
0
1
2
3
Time [ns]

Fig. 3

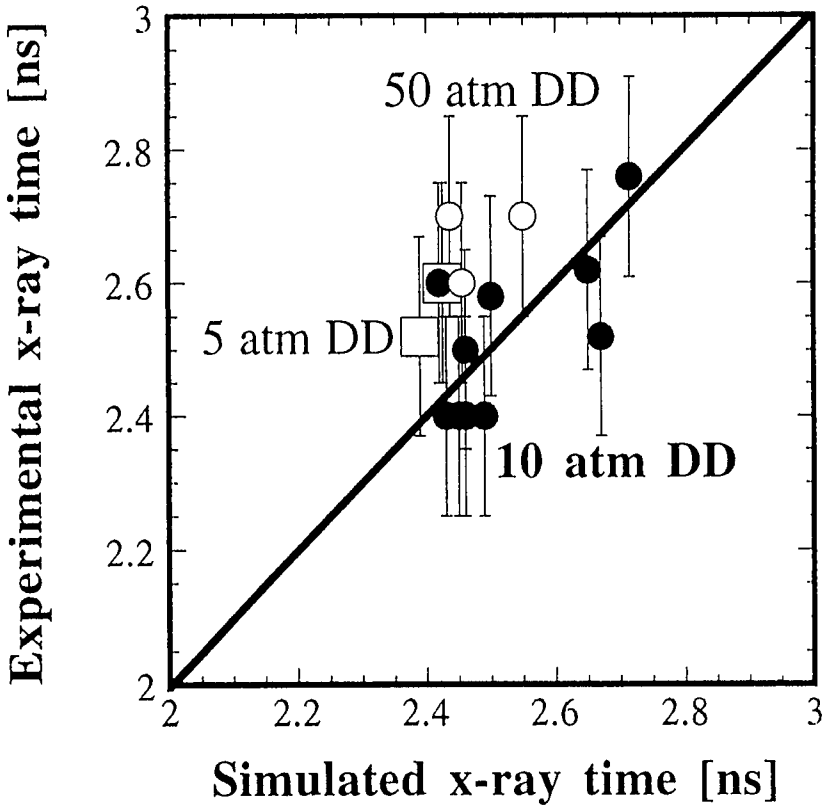
Experimental x-ray time [ns]
Simulated x-ray time [ns]
50 atm DD
5 atm DD
10 atm DD
3
2.8
2.6
2.4
2.2
2
2
2.2
2.4
2.6
2.8
3

Fig. 4(a)

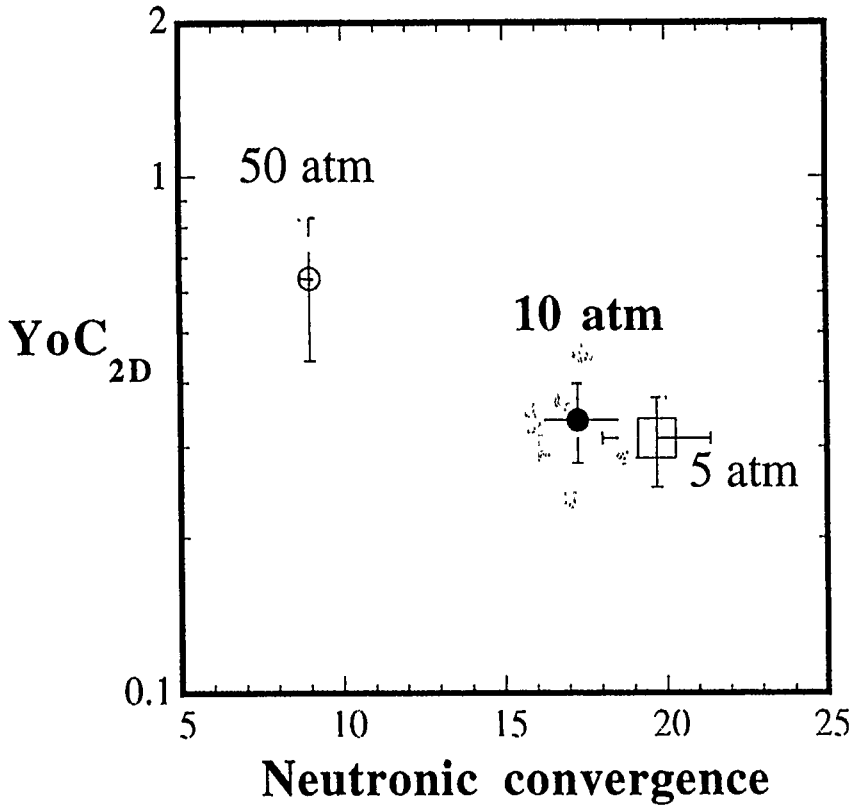
2
1
0.1
50 atm
10 atm
5 atm
YoC2D
5
10
15
20
25
Neutronic convergence

Fig. 4(b)

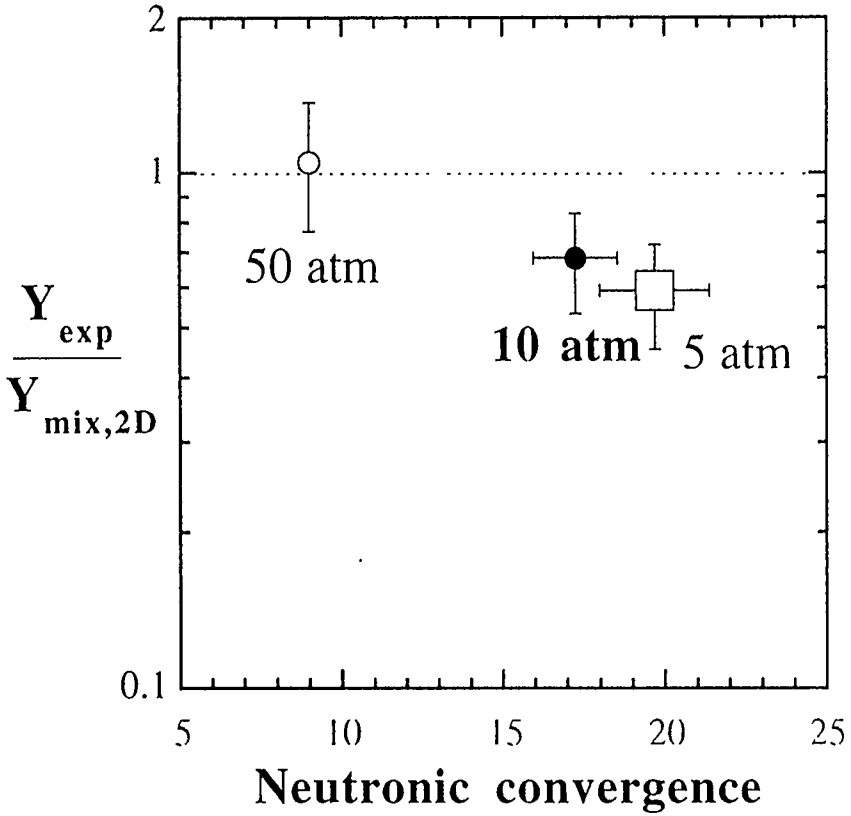
2
1
0.1
5
10
15
20
25
$\frac{Y_{exp}}{Y_{mix,2D}}$
50 atm
10 atm
5 atm
Neutronic convergence

Fig. 5(a)

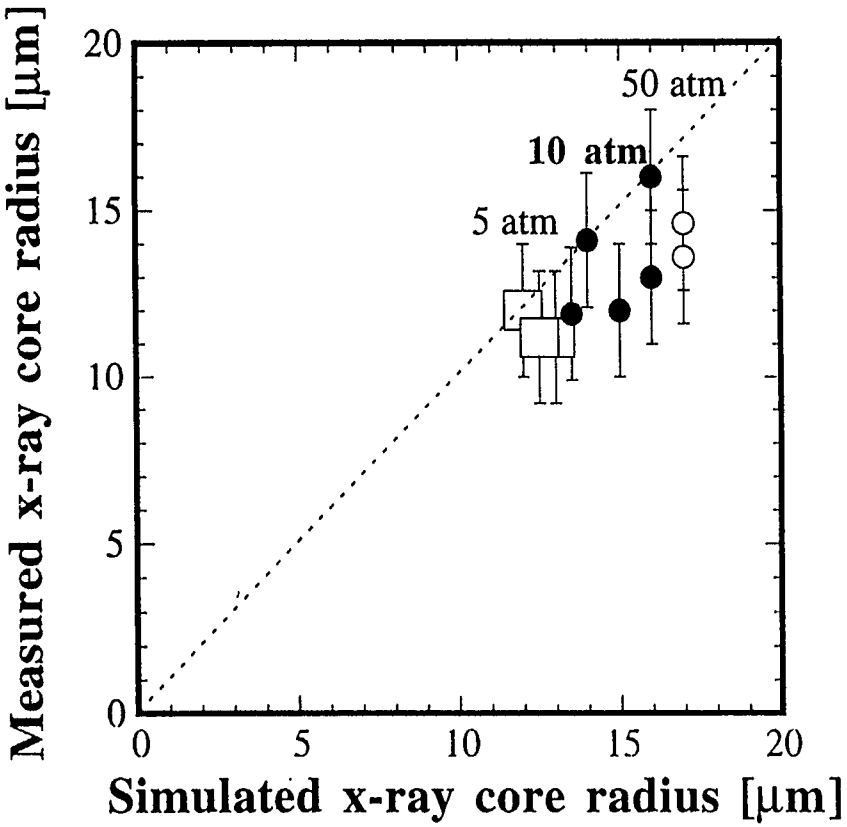
Measured x-ray core radius [μm]
Simulated x-ray core radius [μm]
0
5
10
15
20
50 atm
10 atm
5 atm

Fig. 5(b)

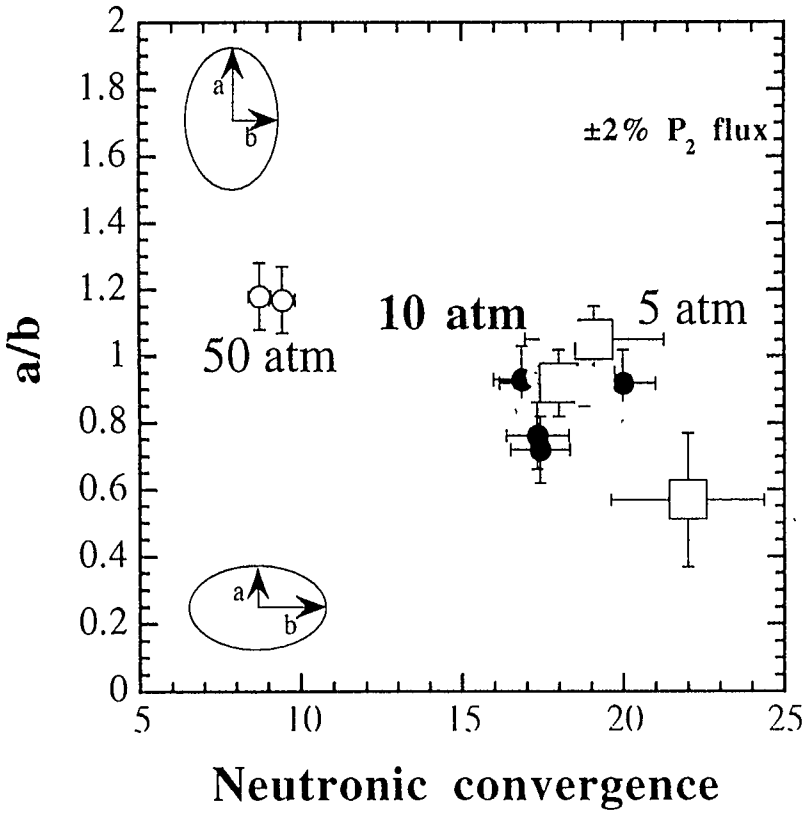
a/b
Neutronic convergence
±2% P2 flux
50 atm
10 atm
5 atm
a
b
a
b
0
0.2
0.4
0.6
0.8
1
1.2
1.4
1.6
1.8
2
5
10
15
20
25